MODELS OF DYNAMIC CORONAL LOOPS

Giovanni Peres
Dip. di Scienze Fisiche ed Astronomiche, Sez. di Astronomia - Piazza del Parlamento 1 - 90134 Palermo - ITALY

September 11, 1999

Abstract. This paper reviews the basic ideas underlying one-dimensional fluid dynamic models of coronal loops and presents some of their most recent applications. These models are an important theoretical support to explore the new scenario provided by the data of Yohkoh, SOHO and TRACE, and are useful to interpret observations, when supplemented by appropriate spectral synthesis codes. Possible developments are also discussed.

Keywords: corona, dynamics, MHD, coronal morphology

1. INTRODUCTION

Since the beginning of X-ray coronal observations it has been recognized that the X-ray and XUV emitting corona is entirely made of plasma magnetically confined in loops (Vaiana, Krieger and Timothy, 1973).

The data from the new satellites - mainly Yohkoh, SOHO and TRACE - are showing us the extent to which the corona is variable, on many time and spatial scales. It is worth noting that, while many of the loops observed are variable and dynamic, the vast majority appears relatively steady, on the basis of their characteristic times, as discussed below in more detail.

The interesting new scenario given us by the recent data has revived the interest for the models of dynamic coronal loops. The scope of the applications of such models is quite broad and includes large dynamic events (e.g. flares) and small ones (microflares, loop brightenings, etc.), the slow evolution of loop plasma and studies of stability; they can be applied to a large fraction of the solar coronal phenomena.

The models of dynamic loops have been, and are, used both to explore theoretically the complex dynamics and thermal evolution of the confined solar corona, and as tools for an accurate interpretation of the data, a non-obvious task given the intricate interplay of the various physical effects.

In the following I will concentrate on the time dependent fluid dynamic models of the coronal loops. Section 2 of this paper will address the fundamental concepts, section 3 will contain a short classification of the models, section 4 will describe some examples of recent results, indicative of the broad scope of activity in this field, including a detailed modeling of a loop brightening observed with TRACE, section 5 will draw the conclusions.

2. WHY 1-D LOOP FLUID MODELS

The mean free path of particles in the coronal plasma ($\approx 10^7$ cm) is typically much smaller than the loops length from one footpoint to the other, allowing a fluid treatment. Also, the plasma is frozen to the magnetic field and since the corona and transition region are typically at a low $\beta = p/(B^2/8\pi)$ (i.e. the magnetic pressure is much higher than the plasma thermal pressure), the plasma dynamics is dominated by the magnetic field and the plasma macroscopic motion can occurr practically only along the magnetic field lines. Also thermal conduction, due to the electron diffusion, occurs only along the field lines - being much less effective across them (Spitzer, 1962). Therefore each plasma loop is independent from the neighbouring ones (Rosner, Tucker and Vaiana 1978) and the dynamics and thermal evolution of the coronal plasma therein is one-dimensional, along the field lines.

For most of the loops, or the systems of loops, made of magnetically confined plasma the Alfven travel time $t_A = L/V_A$ (where L is the characteristic field line length and $V_A = B/\sqrt{4\pi\rho}$ the Alfven speed, with B the magnetic field and ρ the plasma mass density), is much shorter than the plasma evolution time (e.g. the radiative or conductive cooling times, or just the observed evolution time) implying that in most loops the magnetic field structure does not change during the plasma evolution. For instance $t_A \approx 10\ s$ for a loop with $L = 10^9 cm$, $B = 100\ G$, and $\rho = 2 \times 10^{-14}$ g cm^{-3}, i.e. typical coronal values.

These considerations lead us to consider each magnetic flux tube as a rigid and steady container of the plasma, unless in presence of magnetic field changes occurring within few Alfven times; in practice almost each loop behaves as a rigid pipe filled with coronal plasma.

These model assumption can even apply to events characterized by an evolving magnetic field, *after* the structures have stabilized; possible examples are reconnecting loops, after the reconnection is over, or forming loops arcades after morphological changes are over.

On the other hand since each magnetic loop, or even each magnetic "fiber" forming a loop, is independent from the others, the single loop model can be properly applied to those loops in which the various fibers appear to behave coherently; for more complex cases one may consider multiple loop models (e.g. Hori et al., 1997). In this respect the structure of the solar atmosphere, across the field line is of fundamental importance, being dictated possibly by the mechanisms of energy release, as recognized by Litwin and Rosner (1993).

The model, in order to treat satisfactorily the fluid behaviour of the plasma, has to include the mass, momentum and energy conservation equations for the fluid plasma, plus the gas equation of state.

$$\frac{\partial n}{\partial t} + \nabla \cdot (n\mathbf{v}) = 0 \tag{1}$$

$$\frac{\partial (n\mathbf{v})}{\partial t} + \nabla \cdot (n\mathbf{v}\ \mathbf{v}) = -\frac{1}{m}\nabla p + n\mathbf{g} \ , \tag{2}$$

$$\frac{\partial u}{\partial t} + \nabla \cdot [(u+p)\mathbf{v}] = mn\mathbf{g} \cdot \mathbf{v} - n^2 P(T) + \mathcal{H}(\mathbf{r}) + \nabla F_c \, , \tag{3}$$

Where n is the number density of Hydrogen, $\mathbf{v}$ the macroscopic velocity of the plasma, p the plasma pressure, m the average particle massa, g the gravitational acceleration, u the plasma energy density, $P(T)$ the plasma radiative losses per unit emission measure, $\mathcal{H}(\mathbf{r})$ the heating, here prescribed per unit volume, and ∇F_c is the divergence of the heat flux; t and $\mathbf{r}$ are time and the spatial coordinate.

Beyond fluid dynamics, including pressure gradient and gravity components along the field lines, other fundamental physical effects are the thermal conduction, the optically thin radiative losses prescribed according to a spectral model (for example Raymond and Smith, 1977; Cook et al., 1989; Mewe, Lemen, and van den Oord 1986; Kaastra, J.S. 1992; Mewe, Kaastra and Liedahl, 1995 and references therein) and the effect of the heating.

The heating - which maintains the corona at a temperature of million degrees and whose variation may be responsible of many of the observed changes - is a fundamental component of any coronal model and its formulation may depend on the specific problem. In the light of our ignorance of the heating mechaninsm, it may be prescribed as a function of the spatial coordinate and time: for instance it can be assumed uniform in corona or concentrated in some parts of the loop, to mimic different mechanims, as in Antiochos et al. and by Reale et al. discussed below. The heating can be assumed to evolve in various ways, for instance fluctuating in time to simulate microflares (Peres, Reale and Serio, 1993) or rapidly raising in time and decaying after some time. There are also attempts to model in detail specific mechanisms, for instance, in order to model flaring loops, time dependent electron beam heating have been adopted according to the formulation, as in Nagai and Emslie (1984).

Some effects not always taken into account in the models are the effect of hydrogen ionization, which may be important in the energetics and dynamics of the lower transition region, and the plasma compressional viscosity. Albeit viscosity is not crucial in determining the large scale dynamics of the confined plasma, it is important for the plasma dynamics in the presence of shocks, such as those which develop in flaring loops, and for high resolution spectra synthesized from flaring loops, such as the Ca XIX complex around 3.18 A (Peres and Reale, 1993).

In some cases these models have been uses to explore the relevance of plasma effects, such as departure from the Spitzer's formulation of thermal conduction (Karpen, De Vore, 1987; Peres et al., 1987b), in determining the confined plasma dynamics. Incidentally, the above effect appears to be important mostly during the early flare phases which however are characterized by a low emission measure, making any related signature relatively hard to detect.

The numerical solution of the system equations is fundamental to treat realistic cases because the loop plasma evolution depends on several physical effects, all important and at work simultaneously, and many of them are non linear. Additional complexity comes from the formulation of the coronal radiative losses, sometimes approximated as piecewise power laws as, for instance in Rosner, Tucker and Vaiana (1978) or available as a lookup table. Furthermore, one typically needs the freedom to be able to use alternative heating formulations. All the above make an analytical solution of the equations not viable.

The various authors which have undertaken loop plasma fluid modeling have used different numerical schemes. Certainly a very accurate numerical scheme is in order if one is looking for rather subtle effects, e.g. small scale details of plasma dynamics or the fine structure of propagating waves since the results may be easily affected by a coarse numerical scheme; however it may happen that a model uses a highly refined numerical scheme with a coarse atmospheric model or a coarse treatment of the physical effects. An accurate model requires an accurate treatment of the physical effects and of the initial atmosphere as much as an accurate numerical scheme.

The initial conditions of the confined atmosphere may depend on the specific problem. Many studies address the evolution starting with stationary (or even static) initial atmosphere, either generated by a dedicated code or obtained through the relaxation of an approximately hydrostatic initial configuration (see, for instance, Antiochos et al., 1999, in the following).

Also, the presence of the chromosphere and its evolution are important for the loop dynamic model, even if one is just interested to the coronal plasma evolution. The chromosphere, in a rather broad sense, acts as a mass source and as a heat flux sink for the corona and transition region. Furthermore it stabilizes the entire confined atmosphere as it was ascertained through the work by Antiochos (1979), Habbal and Rosner (1979) and Peres et al. (1982). In this respect, one cannot put the loop lower boundary in the lower corona or in the transition region.

The chromosphere is optically thick to its own radiation; however, on the basis of accurate models of the chromosphere and of its radiative losses, it has been possible to ascertain that, if one is interested only to the energy balance and dynamics of the chromosphere, and not to its detailed spectrum, then its radiative losses can be conveniently approximated as effectively optically thin, considerably simplifying the calculations. A piecewise power law formulation of such losses was derived by Peres et al. (1982), on the basis of the Vernazza, Avrett and Loeser (1981) models of chromosphere; McClymont and Canfield (1983) proposed an analogous formulation of the chromospheric losses, also on the basis of Vernazza, Avrett and Loeser (1981). More recently Kankelborg et al. (this issue), has proposed another formulation based on the more updated chromosphere models of Fontenla, Avrett and Loeser (1990).

Another aspect of the hydrodynamic modeling of loops, and more in general of astrophysical plasmas, is the adequate comparison with observations. The ever increasing quality and quantity of the data, the high level of refinement in the models, and the need to produce more and more detailed results on the coronal plasma dynamics requires the synthesis of the emission in specific lines or bands of interests, from the computed evolution of the temperature, density and velocity of the plasma (e.g. Peres et al., 1987a; Reale et al., 1988; Priest, 1998; Hori et al., 1998). The approach by Maggio et al. (1994) is one of the most systematic in this respect; it has produced an environment, written in IDL, open to include new spectral codes and features of new observing instruments. It allows the synthesis of the results of models in the desired format, including that of the relevant observations.

3. A SIMPLIFIED CLASSIFICATION OF THE MODELS

Over the years several groups have developed several one-dimensional fluid dynamics loop models and tackled different problems of coronal loops physics. Treating in detail the several codes and the whole scope of their studies is beyond the limits of this paper. However, rather than ignoring them, I will try a rapid overview and a coarse classification, with a list of references.

There are 0-dimensional models which limit themselves to calculating the averaged temperature and density in the coronal loop. The entire corona is described by these two numbers as functions of time. The exchange of mass and heat with the chromosphere is treated through the boundary conditions. The disadvantage of these codes is that it is impossible to predict most of the observed features but the advantage is that their simplicity allows to compute many cases quite simply and rapidly. These models have been used to study microflaring loops (Kopp and Poletto, 1993; Cargill 1994; Cargill and Klimchuck, 1997)

Then there are models which treat in detail the chromosphere and the photosphere. Studying in detail a flare in the low atmosphere and predicting the relevant spectra requires to calculate both the time dependent hydrodynamics and the radiative transfer in the evolving chromosphere. The group which included Canfield, McClymont and Fisher, along with other collaborators, then at the California University, developed a code and published several papers, mainly McClymont and Canfield (1983a, 1983b), Canfield, Fisher and McClymont (1983), An et al. (1983), Fisher, Canfield, McClymont (1985a, 1985b, 1985c), on the modeling of chromosphere in flaring coronal loops, using a probabilistic escape treatment of radiative transfer. More recently Abbett and Hawley (1999) have developed a new model, discussed below in more detail.

Most of the codes, however, have been dedicated to study the corona and the transition region, often treating the chromosphere in an approximate way. Any attempt to review the results produced would require more space than can be taken by this review. I will try to credit the scientist involved, to mention some work, from which the curious scholar can find other references. The first to publish a model of this kind was Nagai (1980), who showed the feasibility of the chromospheric evaporation. A considerable effort in this field has been invested by the group at the Naval Research Lab., including Cheng et a.(1984), Mariska et al. (1989), Antiochos et al. (1999), Klimchuck (Ofman et al., 1998; Klimchuck and Mariska, 1988). The Palermo group (Peres et al., 1982; Pallavicini et al., 1983; Peres et al. 1987a; Reale et al., 1988; Betta et al., 1997; Peres, 1997) collaborating with the groups of R. Rosner, now in Chicago, and L. Golub at the Center for Astrophysics, in Cambridge has addressed several aspects of loop plasma dynamics and solar and stellar coronal diagnostics. More recently Gan and Fang (1990) and Gan et al. (1991), have developed a hydrodynamic loop code, and Hori et al. (1997) have devised a multi-loop code. Walsh et al. (1997) have paid attention to effects of the pulsed heating in coronal loops; Kankelborg and collaborators (this issue) is working at a model including recent develpments on thermal conduction and radiative losses in the transition region.

Incidentally, let us note that as important as the study of dynamical evolution is that of the stationary conditions of loops. A good knowledge of stationary loop conditions is important per se and because it provides the initial conditions, crucial for a correct determination of dynamic evolution. Static loop models were first studied by Rosner, Tucker and Vaiana (1978) and Vesecky, Antiochos and Underwood (1979). Then Serio et al. (1981) studied loops in hydrostatic conditions, higher than their pressure scale height and subject to non-uniform heating and found the relevant scaling laws. A recent tratment along this line is in Steele and Priest (1994). A more complete model is that of siphon flows in loops, to some extent related to the work of Antiochos et al. (1999) discussed below. For a recent and very detailed model of siphon flow loop we refer to Orlando, Peres and Serio (1995a; 1995b) and references therein.

4. EXAMPLES OF RECENT RESULTS

In the following, three examples of loop hydrodynamic modelling will be shown to illustrate the range of physical problems addressed with these models. The first example studies the evolution of the chromosphere and of its spectrum during a flare; the second deals with the formation of a quiescent prominence knot, namely of cold plasma in the corona; the third studies a loop brightening, i.e. a phenomenon of the hot corona, and the detailed fitting of the related TRACE observations.

4.1. MODELING THE CHROMOSPHERE AND PHOTOSPHERE

Abbett and Hawley (1999) have just published a paper on their new loop model which deals with the time dependent hydrodynamics and radiative transfer in the lower atmosphere, plus the due attention to the corona and transition region.

Abbett and Hawley study three cases of electron beam heated flaring chromosphere, the fundamental difference being the input energy flux: 10^9, 10^{10} and 10^{11} erg s^{-1} cm^{-2}, respectively. The beam of non-thermal electrons has a power law energy distribution with a lower energy cutoff at 20 KeV and an index of -5.

The case of intermediate energy flux carries all the important physical features the authors want to show and is briefly discussed here. Fig. 1 shows the temperature, density of electrons and of mass along with the electron beam heating and the Hydrogen ionization fraction vs. height in the chromosphere at three moments of the early flare evolution. The initial flare phase is characterized by a gentle evolution; at later phases, approximately 25 s since the heating has started, the atmosphere cannot radiate any more the input power and evolves explosively. Fig. 2 shows the explosive phase of the flare.

The authors study in detail the lines and continuum formation in the atmosphere. Fig. 3 shows the H_α and the Ca II K spectral lines at selected times of the flare evolution, synthesized from the chromosphere model. The line shapes remain simmetric during the early, gentle, phase but become strongly non-symmetric in the later explosive phase characterized by a very dynamic and complex atmospheric evolution.

The case with a flux ten times smaller than the one discussed above never gets explosive, whereas the case with a flux ten times larger goes explosive in a fraction of a second. It is also worth noting that the X-ray heating is never important in each of the cases Abbett and Hawley have studied.

4.2. FORMATION OF A QUIESCENT PROMINENCE

Antiochos et al. (1999), have simulated the formation of a prominence condensation in a coronal loop. More specifically they have studied the evolution of a prominence knot, which is just part of a prominence, inside a loop. The idea is that the whole prominence is formed by a set of loops each having a knot in the highest part and, by modeling the formation of one of such knots one can understand, in principle, the formation of whole prominences.

The topmost part of the loop consists of a rather long, almost horizontal branch (infact slightly dipped at the very center of the loop); the rest of the loop on each side has the shape of a quarter of a circle rooted in the lowest atmosphere. The initial conditions consist of a hydrostatic configuration (relaxed from an initial trial configuration).

The key aspect of the simulation is a heating mostly concentrated at the footpoints: more specifically the volumetric heating, prescribed as a function of position, is $E = E_0 + E_1(s,t)$ where $E_0 = 1.5 \times 10^{-5}$ ergs cm^{-3} s^{-1} and $E_1 = 10^{-3}$ ergs cm^{-3} s^{-1} below s_1, the highest point of the chromosphere, and $E_1 = 10^{-3} exp[-(s-s_1)/\lambda]$ for $s > s_1$, and $\lambda = 10^8$ cm. E_1 is ramped up linearly in time over the first 1000 s and then left constant in time.

The loop is assumed to be symmetric and therefore only half of the loop is studied.

Under the effect of the heating, the loop first heats entirely, then the top part starts to cool and condense, as shown in Fig. 4.

Table I. Parameters of the simulations with transient constant heating

Name	Location	H_0 (10^{-3} erg cm^{-3} s^{-1})	s_0 (10^9 cm)	σ (10^9 cm)	Duration (sec)
A	Footpoint	10	0.3	0.05	3000
B	Asymmetric	0.4	3	0.5	3000
C[1]	Asymmetric	0.4	3	0.5	3000

[1] As case B, but constant for the first 100 s and then decaying exponentially with an e-folding time of 300 s.

Fig. 5 shows the very onset of the condensation and the following evolution, with the formation of shock fronts and steep transition regions between the condensation and the rest of the corona. The physical explanation is that the heating concentrated at the loop footpoint drives the plasma evaporation from chromosphere to the corona, where the heating is insufficient and hence the loss of equilibrium leading to the condensation.

Antiochos et al., have been able to solve this problem thanks to a new code with second order Godunov scheme, and a particular adaptive mesh scheme which allowed them to follow the evolution of the sharp fronts due the condensation.

It is worth noting, also, that Serio et al. (1981) already suggested an analogous mechanism as responsible for the prominence formation, during the long term evolution of magnetic loops from the compact magnetic configuration of active regions to the more extended one of old regions hosting filaments. According to Serio et al., (1981) such an evolution would be energetically more convenient, with respect to the case with maximum temperature at the loop apex, if the heating is concentrated at the loop base.

4.3. MODELLING AS A DIAGNOSTIC OF THE HEATING

Along the same line of thought, Reale et al. (2000a, 2000b) show that the detailed hydrodynamic/thermodynamic modeling of a loop brightening, observed with TRACE at a high angular and temporal resolution leads to crucial insight on the location and timing of the heating driving the loop brightening. TRACE observed AR 8253, then very close to the solar disk center, on June 26, 1998, taking one frame every 30 seconds over a few hours, in the 171 A band; the pixel size is half an arcsecond.

The loop gets bright initially at the footpoints. Then from each footpoint, bright, sharp fronts expand gradually along the loop; first from the northern footpoint, ≈ 10 min. since the initial brightening and further 7 min later from the southern footpoint. The brightness fronts propagate at an apparent speed of 100 Km/s. The surface brightness along the loop is always definitely asymmetric, with the northern footpoint and leg brighter than the southern ones. Fig. 6 shows the region where the loop brightened with the loop clearly visible.

Reale et al. inferred from the images that the loop, inclined on the solar surface by 60 degrees, is approximately semicircular, the footpoints distance being $\approx 10^{10}$ cm, with an almost equal distance between the center of the footpoints and the apex.

The first part of the sequence shows that the loop is not visible in the 171 A band, which detects preferentially plasma around 10^6 K. The authors, therefore, assumed that the plasma is initially at 5×10^4 K and the pressure is 0.01 dyne cm^{-2}, i.e. the loop plasma is at rather low temperature, pressure and density.

Reale et al., have used the Palermo-Harvard 1-D fluid dynamic code (Peres et al., 1982; Betta et al. 1997) to model the brightening; a semicircular loop geometry and a constant cross section have been assumed for the loop; both geometrical assumptions being appropriate to the loop observed. In practice the geometry never changes during the evolution; while many loop subfilaments or threads brighten simultaneously, at the beginning, they all follow the same evolution during the whole rising phase (≈ 3000 sec); later the various subfilaments appear to behave differently. Reale et al. have modelled just the rising phase, to which the model can be applied correctly.

The heating term has been modelled as a separable function of position along the loop and time: the spatial distribution is gaussian and different locations and widths along the loop have been tried, as shown in Table I. The impulsive heating is assumed to turn on and remain constant during the simulation; as discussed in Table I, the last simulation of the set consider an heating with an exponentially decaying tail.

The observation is fitted with the model as follows: first, the loop geometry is derived from the observations, then, the initial conditions of the coronal loop plasma are inferred. Having defined the initial conditions, the intensity, spatial distribution and evolution of the heating are been chosen and the loop plasma evolution is then computed. The emission in the 171 A band is then derived from the plasma density and temperature distribution along the loop during the whole evolution, taking into account also the folding with the instrument spectral response to allow a direct comparison with the focal plane data. The evolution of the synthesized emission is finally compared with observations, considering several characteristics including the brightness contrast between the two footpoints and the time lag between their brightening. From the comparison one can decide if and how to adjust the heating parameters to fit better the observations. The task is to reproduce the observations at best.

In this context, Reale et al. have paid particular attention to the contrast between footpoints and loop apex, and to the relative timing of the brightenings at the footpoints and at the apex. When interpreting the results it should be considered that the 171 A spectral band (as all the TRACE coronal ones) is relatively narrow and the plasma is more easily detected in a narrow temperature range around 10^6 K.

The first model calculation (case A in Table I), consisted of heating one footpoint, since the first brightening occurs at a footpoint; the relevant results are in Fig. 7. The simulations show that the opposite footpoint brightens first because that is the place where the plasma is compressed and the emission measure increases. This case shows how a too straightforward interpretation of observations to derive information on the the heating can lead to wrong results. It is also very important to note that this simulation fails to reproduce observations, because the model predicts that the two footpoints and the two halves of the loop brighten alternatively, while the two footpoints brighten with only a slight time difference, in the observations.

If the heating were located exactly at the loop apex the footpoints would, obviously, brighten simultaneously (at variance with observations). The heating cannot be, therefore, neither at the footpoints nor at the apex.

Therefore, on the basis of the relative brightness contrast between the two footpoints and the timing of their brightening Reale et al. infer that the heating should be somewhere in between, most likely at, approximately, one third of the loop's length, reckoned from one footpoint, and opposite to the footpoint which brightens first. The evolution of the surface brightness in the 171 A band, synthesized from this model (case B in Table I), agrees with observations much better than the simulations discussed before (Fig. 8).

As for the timing of the heating, in all the simulations so far analyzed, heating is turned on suddenly and remains thereafter constant. Also, at late phases of the observed evolution, the observed brightness profile along the loop is flatter than the one obtain in case B. Reale et al. then tried a heating which is suddenly turned on, stays on constantly for 100 s., and then it decays exponentially with an e-folding time of 300 s. They obtain an even better agreement with observations (cf. Fig. 9) and definitely the best fitting, among those tried by Reale et al., of the spatial and temporal distribution of the emission along the loop.

5. CONCLUSIONS

The data collected by the recent coronal instruments are spurring the use of dynamic models of coronal loops and the development of new ones. These models are of fundamental importance to understand the macroscopic dynamics and thermal evolution of confined plasma under the combined effect of several physical mechanisms (including thermal conduction, heating and radiative losses) which act in a complex, non-linear way. As such they serve both as theoretical tools and as a means of interpreting accurately observations.

Within the limited space of this presentation, a sketchy reference to previous work has been presented. Also three very recent studies have been reviewed, in the perspective to show both the theoretical and the interpretative use of the models, as well as the range of application covering three different phenomena and physical conditions occurring in loops: the modeling of the optically thick chromospheric flare (Abbett and Hawley, 1999), the model of prominence formation (cold plasma forming in the corona) by Antiochos et al. (1999), and the modeling of a loop brightening observed by TRACE, yielding insight on the timing and location of the heating (Reale et al., 2000a; 2000b), at least for the specific event.

Each team involved in loop modeling is now addressing some problem in the relevant field and still a lot has to be said on each problems tackled so far. So in the near future one may expect a sizable amount of activity along lines already drawn in the recent past. One may also expect new developments of loop models, e.g. through the exploitation of more advanced numerical techniques (to approximate better the differential equations, to improve the numerical mesh, etc.) or refining the physical effects in the model.

The scope of loop modeling is rather broad and one may foresee many new developments. Just to mention a few of them, TRACE observations clearly show that loops are formed by many filaments (with a cross-field structure down to the resolution limit) which, in some cases, evolve differently; this may require the develoment of multi-loop models like the one by Hori et al. (1997), also, since observations can help to constrain them, it could be time to include more in detail specific heating mechanisms. Furthermore, chemical abundance stratification, or differentiation, in the solar atmosphere is a hot topic and Lenz et al. (1998) has provided a recent view on the problem, amenable to treatment in the loop model context; it is important to determine how the stratification, if present, influences the spectra and, possibly, the confined plasma dynamics through the radiative losses. It is equally important, on the other hand, to understand the extent to which dynamic loop phoenomena may alter any gravitational chemical settling and bring back abundances to their standard average value.

There is a large number of problems in loop physics which have not been solved, observations provide new challenges, and the ever growing computing power grants that we can keep developing more detailed and accurate loop models to tackle the problems. And human ingenuity can lead easily to welcome surprises.

ACKNOWLEDGMENTS

I acknowledge stimulating discussions with, and help by, F. Reale. This work was partially supported by Agenzia Spaziale Italiana and by M.U.R.S.T.

References

Abbett, W.P., Hawley, S., 1999, *ApJ*, 521, 906.
An, C.H., Canfield, R.C., Fisher, G.H., McClimont, A.N., 1983, *ApJ*, 267, 421
Antiochos, S. K., 1979, *ApJL*, 232, L125
Antiochos, S. K., MacNeice, P.J., Spicer, D.S., Klimchuck, J.A., 1999, *ApJ*, 512, 985.
Betta, R., Peres, G., Reale, F., Serio, S., 1997, *A&AS*, 122, 585
Canfield, R.C., Fisher, G.H., McClimont, A.N., 1983, *ApJ*, 265, 507
Cargill, P.J., 1994, *ApJ*, 422, 381
Cargill, P.J., Klimchuck, J.A., 1997, *ApJ*, 478, 799
Cheng, C.-C., Doschek, G. A., Karpen, J. T., 1985 *ApJ*, 286, 787
Cook, J.W., Cheng, C.-C., Jacobs, V.L., and Antiochos, S.K., 1989, *ApJ*, 338, 1176
Fisher, G.H., Canfield, R.C., McClimont, A.N., 1985a, *ApJ*, 289, 414
Fisher, G.H., Canfield, R.C., McClimont, A.N., 1985b, *ApJ*, 289, 425
Fisher, G.H., Canfield, R.C., McClimont, A.N., 1985c, *ApJ*, 289, 434
Fontenla, J.M., Avrett, E.H., Loeser, R., 1990, *Apj*, 355, 700
Gan,W.Q. and Fanc,C., 1990, *ApJ*, 358, 328
Gan,W.Q., Fang,C., and Zhang,H.Q., 1991, *Astr. and Astroph.*, 241, 618
Habbal, S.R., Rosner, R., 1979, *ApJ*, 234, 1113
Hori, K., Yokoyama, T., Kosugi, T., and Shibata, K., 1997, *ApJ*, 489, 426
Hori, K., Yokoyama, T., Kosugi, T., and Shibata, K., 1998, *ApJ*, 500, 492
Kankelborg, C., Longcope, D., Fletcher, L., De Pontieu, B., *Solar Ph.*, this issue
Karpen, J.T., DeVore, C.R., 1987, *ApJ*, 320, 904
Klimchuck, J.A., Mariska, J.T., 1988 *ApJ*, 328, 334
Kopp, R.A., Poletto, G., 1993, *ApJ*, 418, 496
Lenz, D.D., Lou, Y.-C., Rosner, R., 1998, *ApJ*, 504, 1020
Litwin, C. and Rosner, R., 1993, *ApJ*, 412, 375
Maggio A., Reale F., Peres G., Ciaravella A., 1994, *Comp. Phys. Comm.*, 81, 105
Mariska, J.T., Emslie, A.G., Li, Peng, 1989 *ApJ*, 341, 106
McClimont, A.N., Canfield, R.C., 1983a, *ApJ*, 265, 483
McClimont, A.N., Canfield, R.C., 1983b, *ApJ*, 265, 497

Mewe, R., Kaastra, J.S., Liedahl, D.A. 1995, *Legacy*, 6, 16
Mewe, R., Gronenschild, E.H.B.M., and van den Oord, G.H.J. 1985, *A&AS*, 62, 197
Mewe, R., Lemen, J.R., and van den Oord, G.H.J. 1986, *A&AS*, 65, 511
Nagai, F., 1980, *Sol. Phys.*, 68, 351
Nagai, F., Emslie, A.G., 1985, *ApJ*, 279, 896
Ofman, L., Klimchuck, J.A., Davila, J.M., *ApJ*, 493, 474
Orlando, S., Peres, G., Serio, S., 1995, *Astr. and Astroph.*, 294, 861
Orlando, S., Peres, G., Serio, S., 1995, *Astr. and Astroph.*, 300, 549
Peres, G., 1997, *ESA SP-404*, p.55
Peres, G., Reale, F., 1993, *Astr. and Astroph.*, 267, 566
Peres, G., Reale, F., Serio, S., 1993, in "Physics of Solar and Stellar Coronae", J. Linsky and S. Serio (ed.), Kluwer Academic Publishers, p. 151
Peres, G., Reale, F., Serio, S., Pallavicini, R., 1987a, *ApJ*, 312, 895
Peres, G., Rosner, R., Serio, S., 1987b *Il Nuovo Cimento B*, 99B, 29
Peres, G., Rosner, R., Serio, S., Vaiana, G.S., 1982, *ApJ*, 252, 791
Priest, E.R., Foley, C.R., Heyvaerts, J., Arber, T.D., Culhane, J.L., Acton, L.W., 1998, *Nature*, 393, 545
Raymond, J.C., Smith, B.W., 1977, *ApJS*, 35, 419
Reale, F., Peres, G., Serio, S., De Luca, E., Golub, L., 2000a, *ApJ*, in press
Reale, F., Peres, G., Serio, S., Betta, R., De Luca, E., Golub, L., 2000b, *ApJ*, in press
Reale, F., Peres, G., Serio, S., Rosner, R., Schmitt, J.H.M.M., 1988, *ApJ*, 328, 256
Rosner, R., Tucker, W.H., Vaiana, G.S., 1978 *ApJ*, 220, 643
Serio, S., Peres, G., Vaiana, G.S., Golub, L., Rosner, R., 1981, *ApJ*, 243, 288
Spitzer, L., *Physics of fully ionized gases.* Interscience, New York, N.Y., 1962
Steele, C.D.C, and Priest, E.R., 1994, *Astr. and Astroph.*, 292, 291
Vaiana, G.S., Krieger, A.S., Timothy, A.F., 1973, *Solar Phys.*, 32, 81
Vernazza, J.E., Avrett, E.H., Loeser, R., 1981, *ApjS* 45, 635
Vesecky, J.F., Antiochos, S.K., and Underwood, J.H., 1979, *Apj* 233, 987
Walsh, R.W., Bell, G.E., Hood, A.W. *Sol. Phys.*, 171, 81

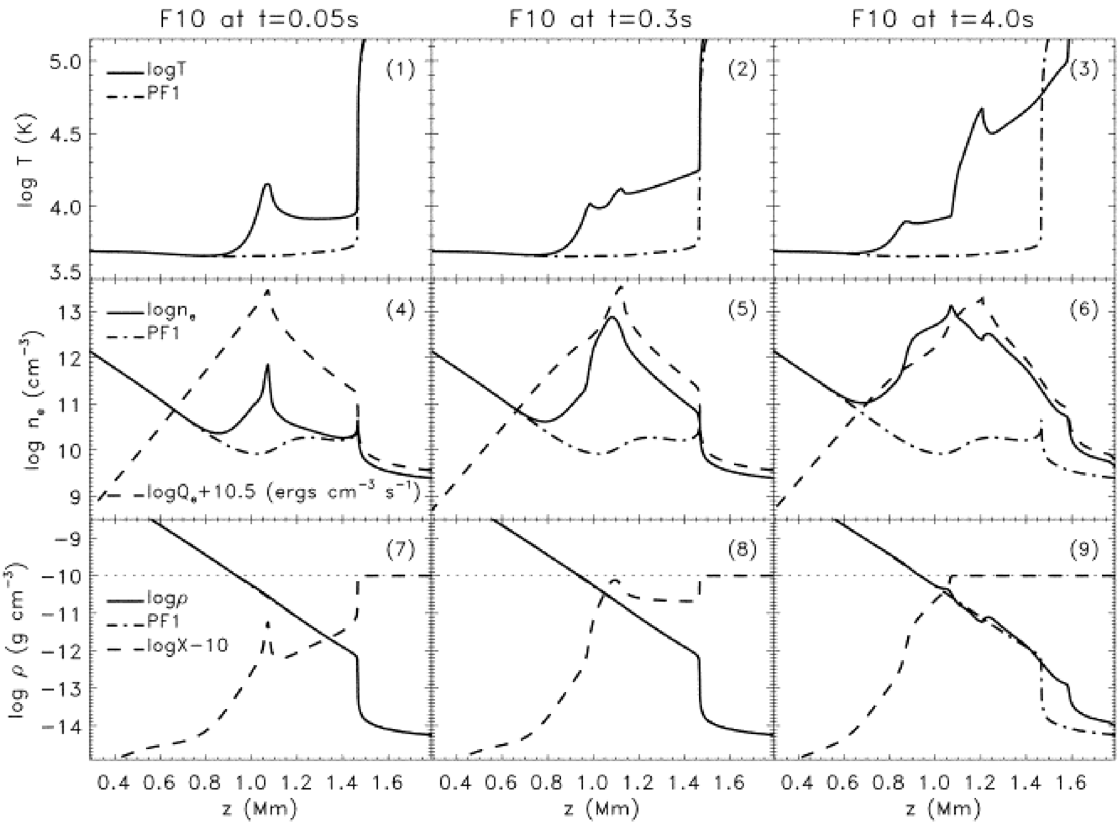

Figure 1. The low solar atmosphere during the early, gentle phase of electron beam heated flare evolution. The figures show the temperature (top row), electron density and electron beam heating per unit volume (middle row), the mass density and the Hydrogen ionization fraction vs. height at selected times vs. height in the chromosphere. In each panel the dot-dashed profile (PF1) is the initial atmospheric profilei and the dotted line marks the level to which Hydrogen is fully ionized (From Abbett and Hawley, 1999).

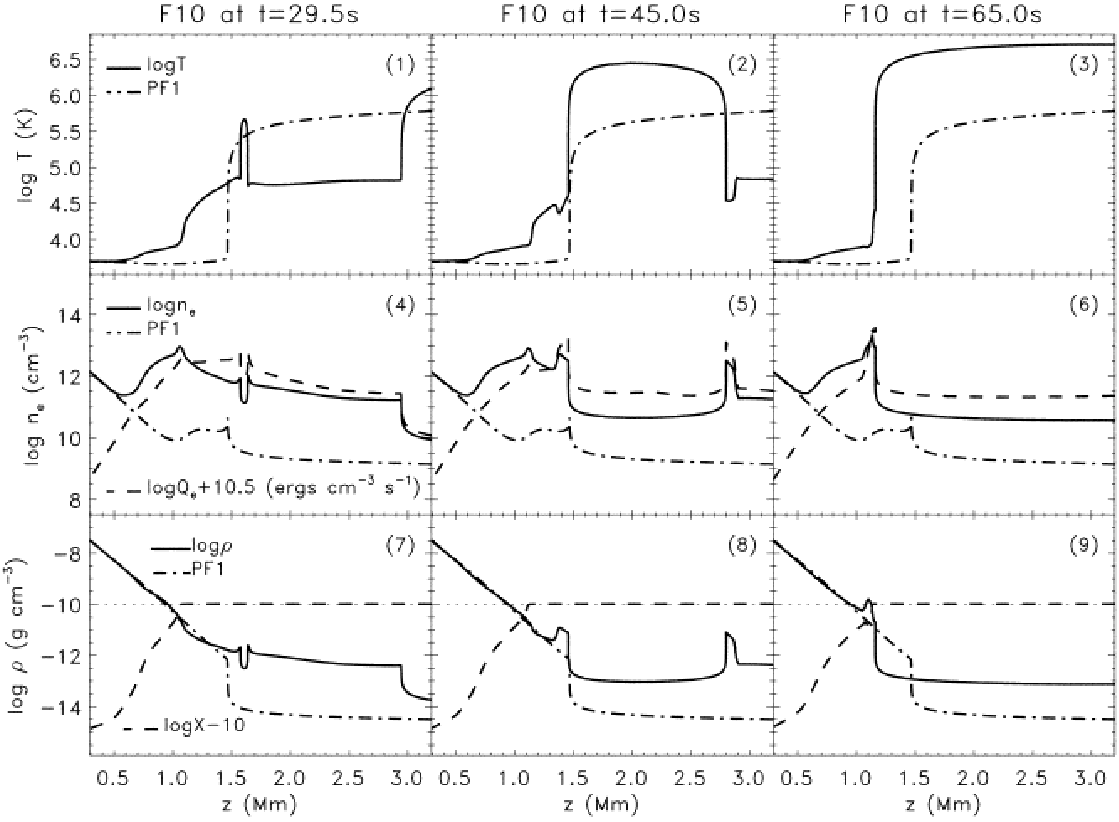

Figure 2. The atmosphere during the later, explosive phase of evolution. The notation is the same of Fig. 1. (From Abbett and Hawley, 1999).

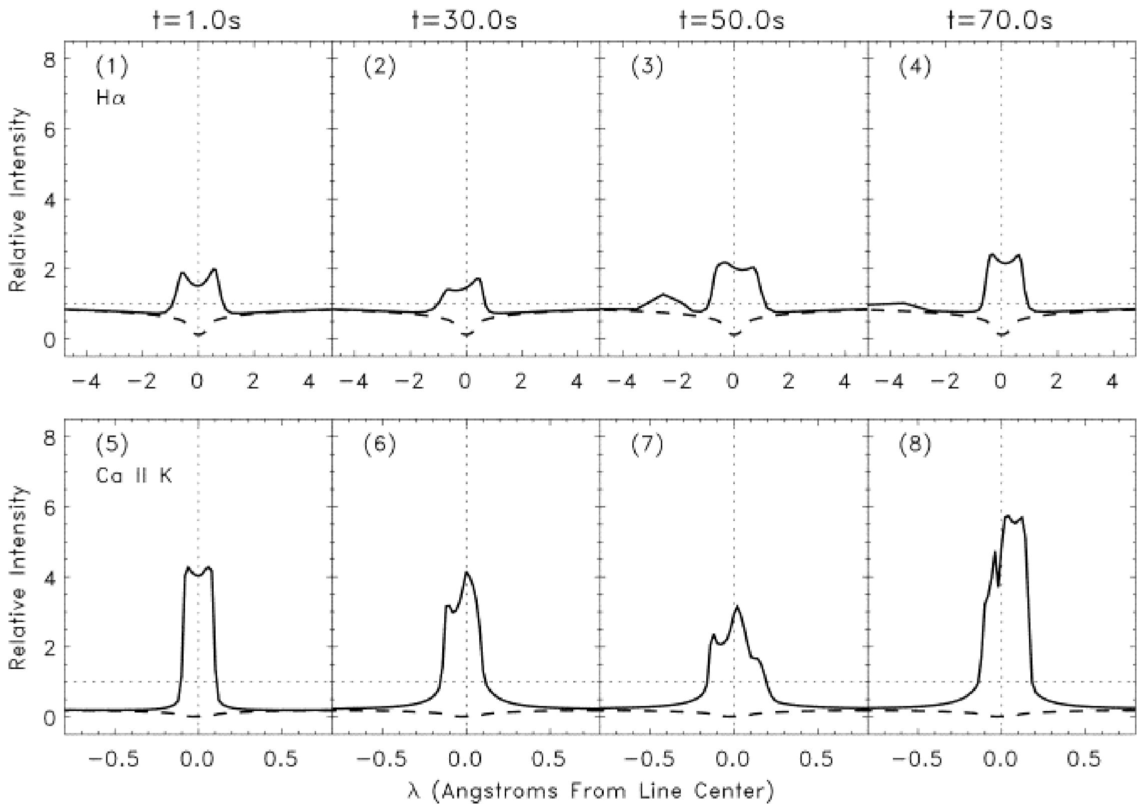

Figure 3. Evolution of the H_α (top row) and the Ca II K (bottom row) spectral lines during the flare. The intensity is relative to the continuum and the dashed line marks the preflare line profile. (From Abbett and Hawley, 1999).

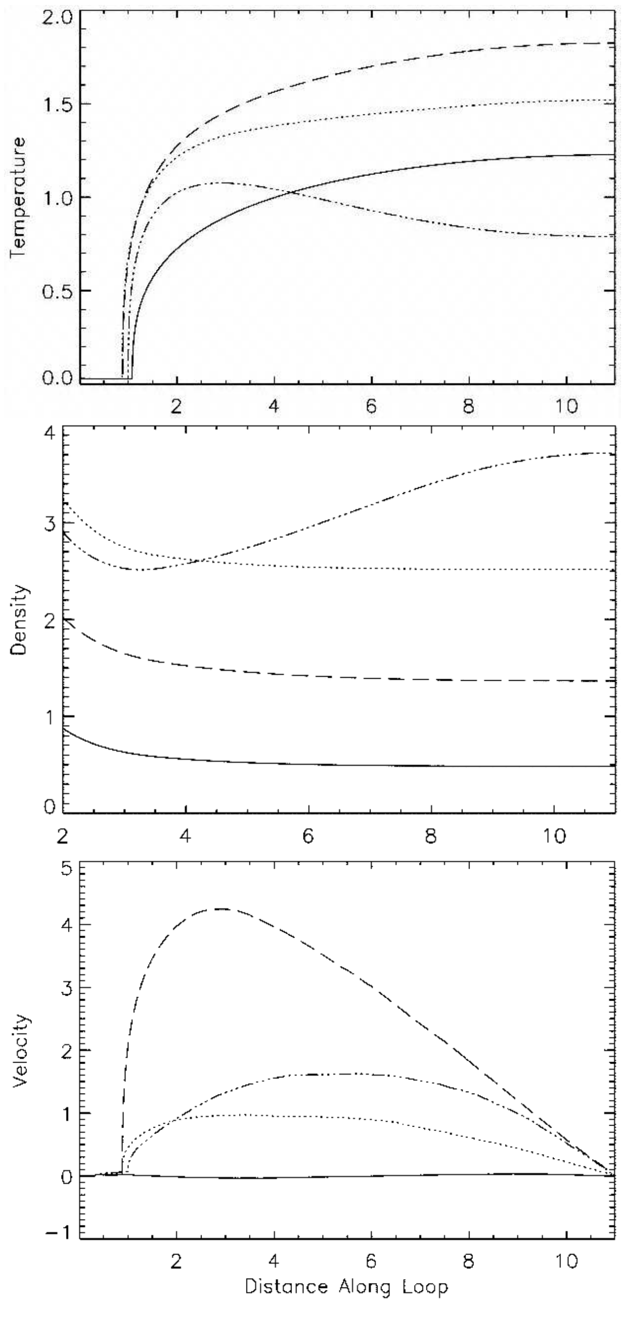

Figure 4. Temperature (top panel) in units of 10^6 K, number density (middle) in units of 10^9 cm^{-3}, and velocity (bottom) in units of 10^6 cm s^{-1}, vs. distance from the loop base (in units of 10^9 cm), at selected times during the evolution before the formation of the condensation. The solid curves correspond to $t = 0$ s, the dashed ones to $t = 10,000$ s, the dotted ones to $t = 30,000$ s, and the dash-dotted ones to $t = 50,000$ s. Note that the middle panel has not the same spatial scale as the other two, showing just the part of the loop above the chromosphere. (Adapted from Antiochos et al., 1999).

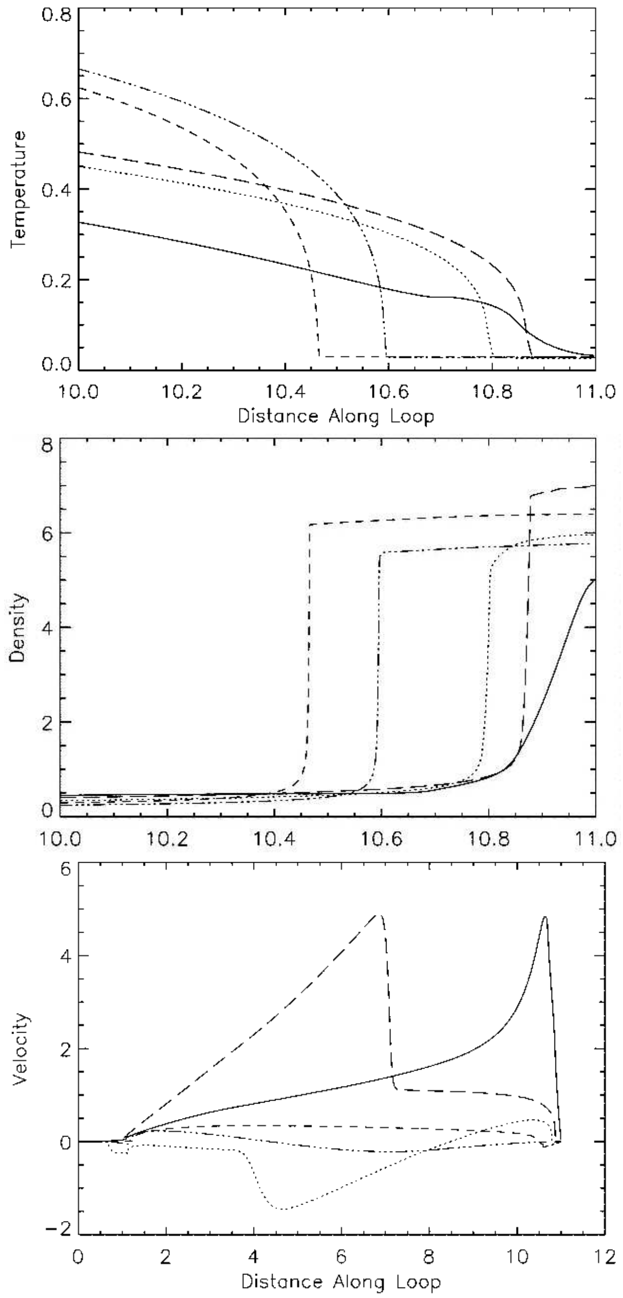

Figure 5. The analogous of figure 4 but after the condensation phase has begun; the two topmost panels refer just to the part near the loop midpoint, the bottom one to the entire half-loop. The solid curves correspond to $t = t_o =$ 54,000 s, when the condensation first appears; the long dashed ones to $t = t_o +$ 500s, the dotted ones to $t = t_o +$ 1000 s, the dash-dotted ones to $t = t_o +$ 10,000 s, and the short dashed ones to $t = t_o +$ 30,000 s. (Adapted from Antiochos et al., 1999).

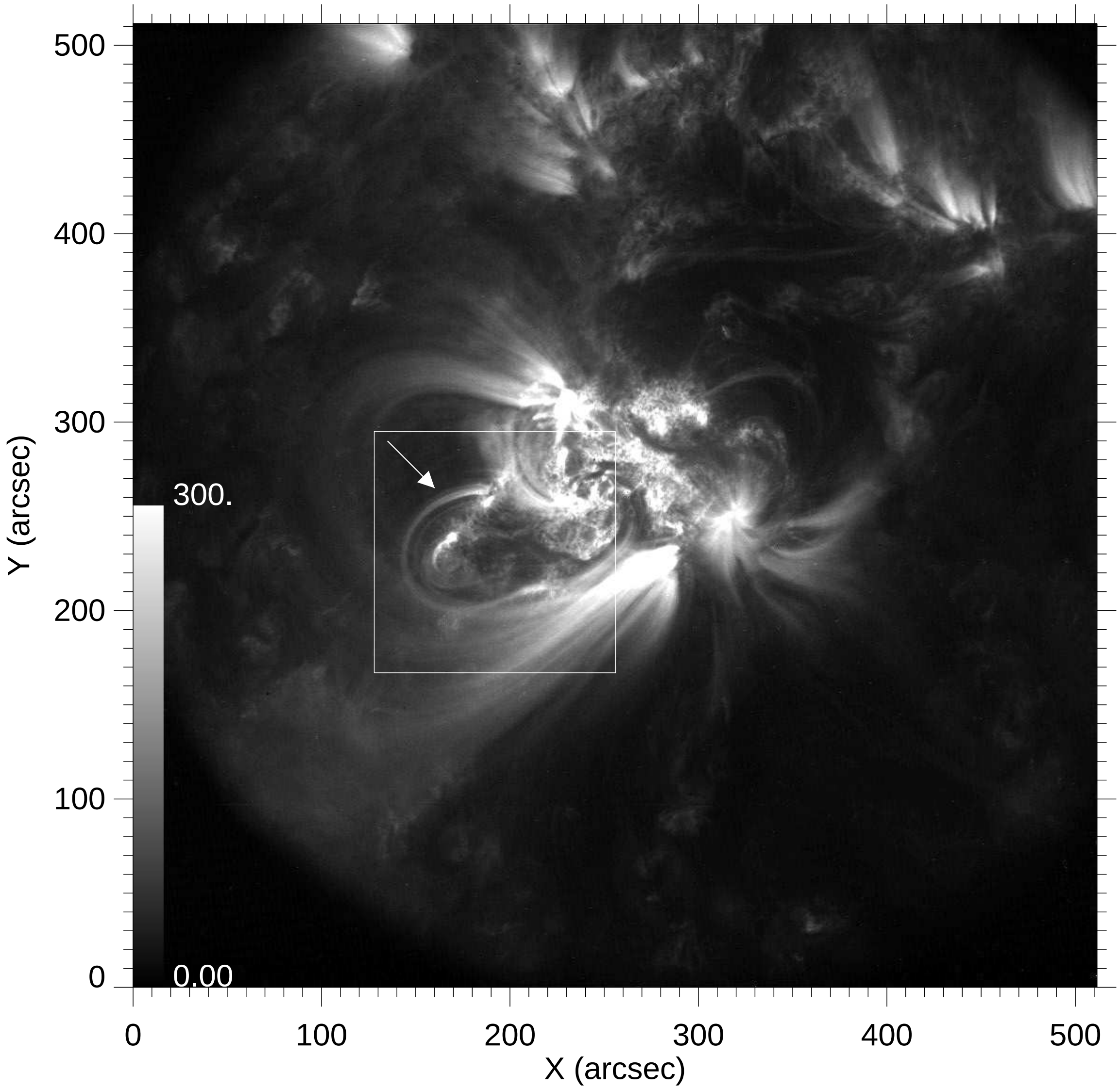

Figure 6. Whole field of view of the TRACE observation in the 171 Å band, made at 13:54:17 UT. The exposure time is 23 s and the brightness scale units are Digital Numbers. The square encloses the region where the loop appeared. The loop itself, already clearly visible in this image, is marked with an arrow (From Reale et al., 2000a).

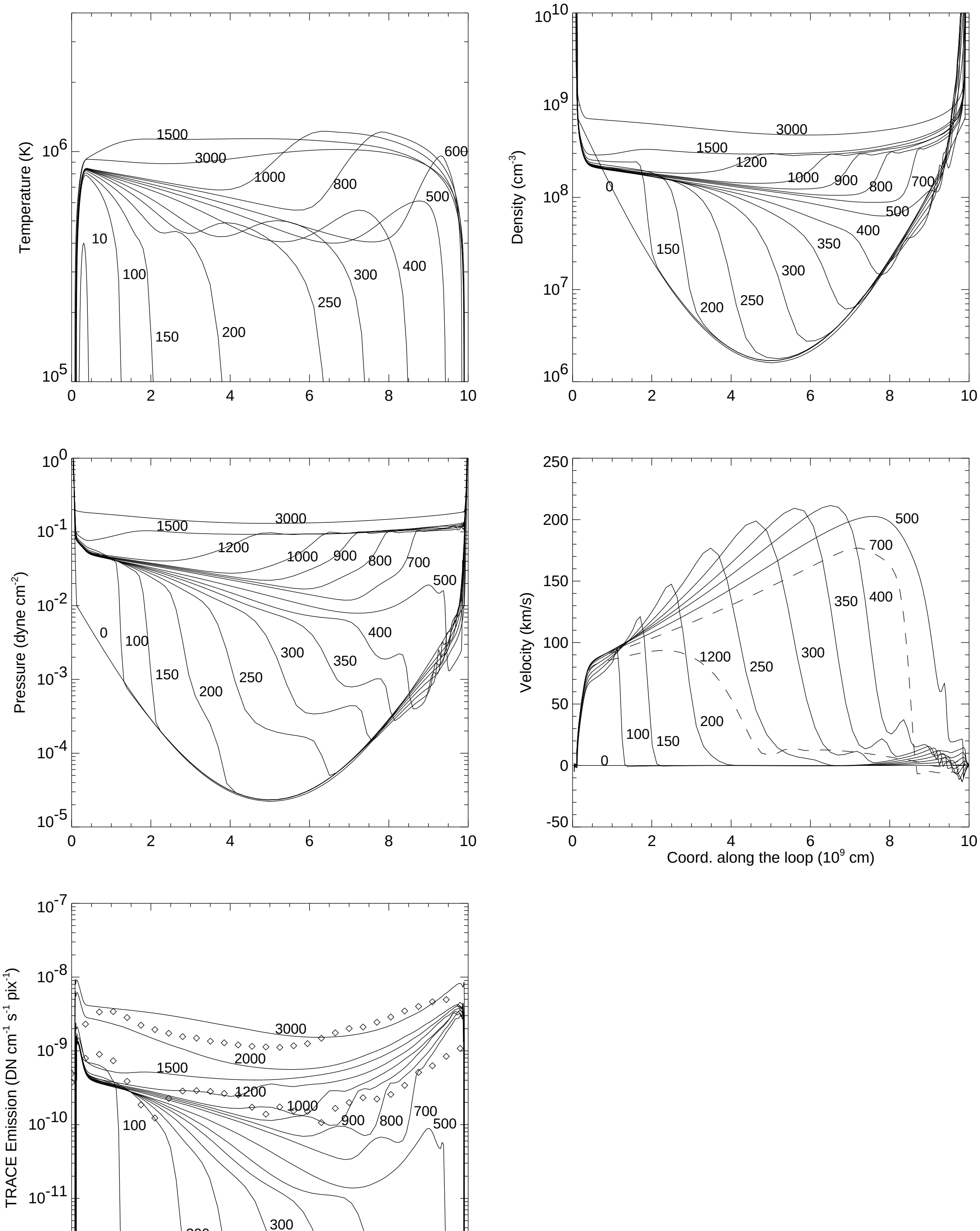

Figure 7. Plasma temperature, density, pressure, velocity and emission per unit volume in the TRACE 171 Å band, vs. the spatial coordinate and time, for the model loop heated at the left footpoint (Model A in Table 1). Time (in seconds since the start of the heating) is shown by each curve. To avoid confusion, velocity curves after 500 sec are dashed. The lowest left panel shows the observed brightness distributions (*diamonds*) at t=1875 s (lower) and at t=3374 s (upper) (From Reale et al., 2000b).

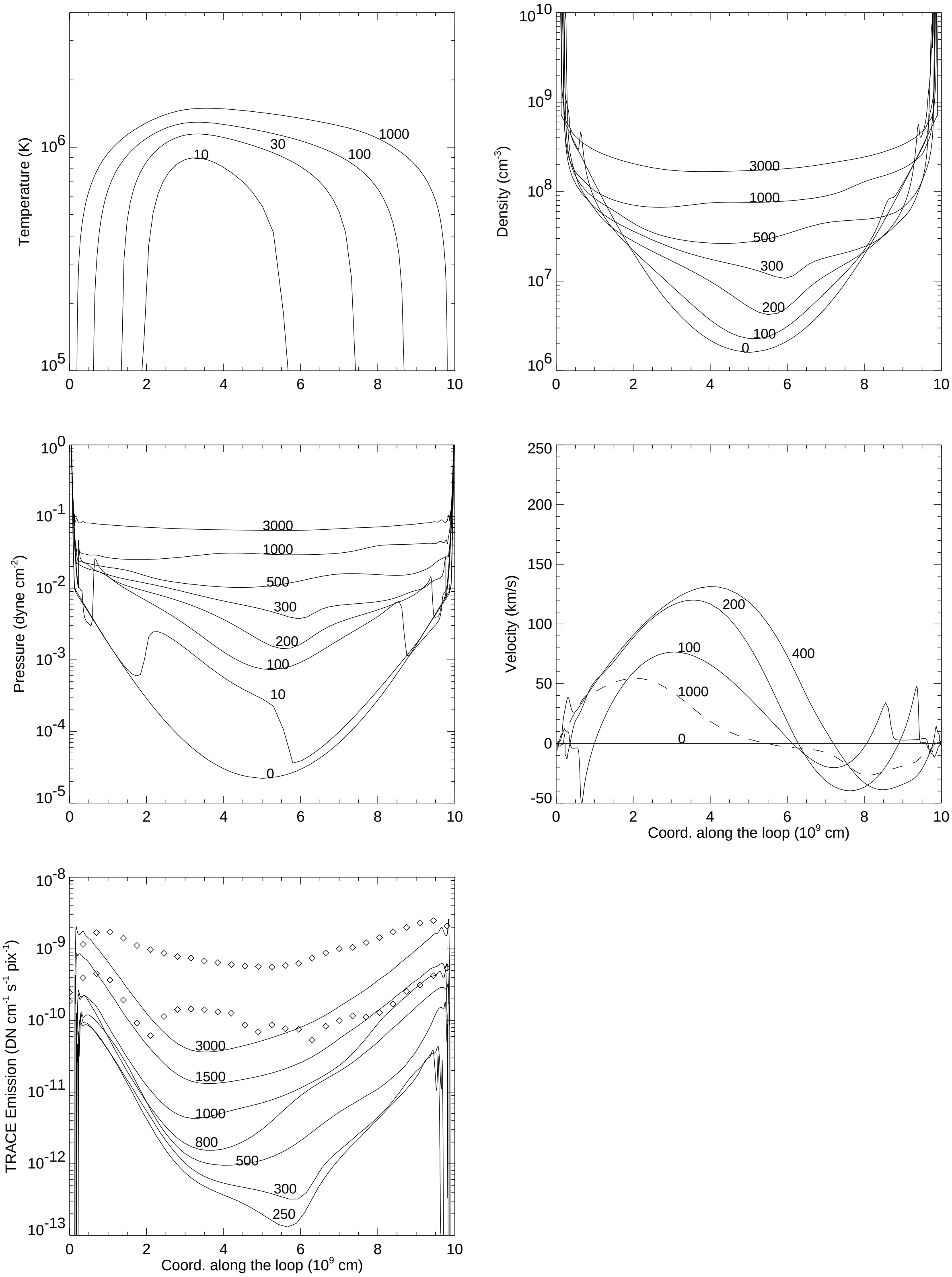

Figure 8. As Fig.7 for the model loop heated asymmetrically on the right leg (Model B in Table 1) (From Reale et al., 2000b).

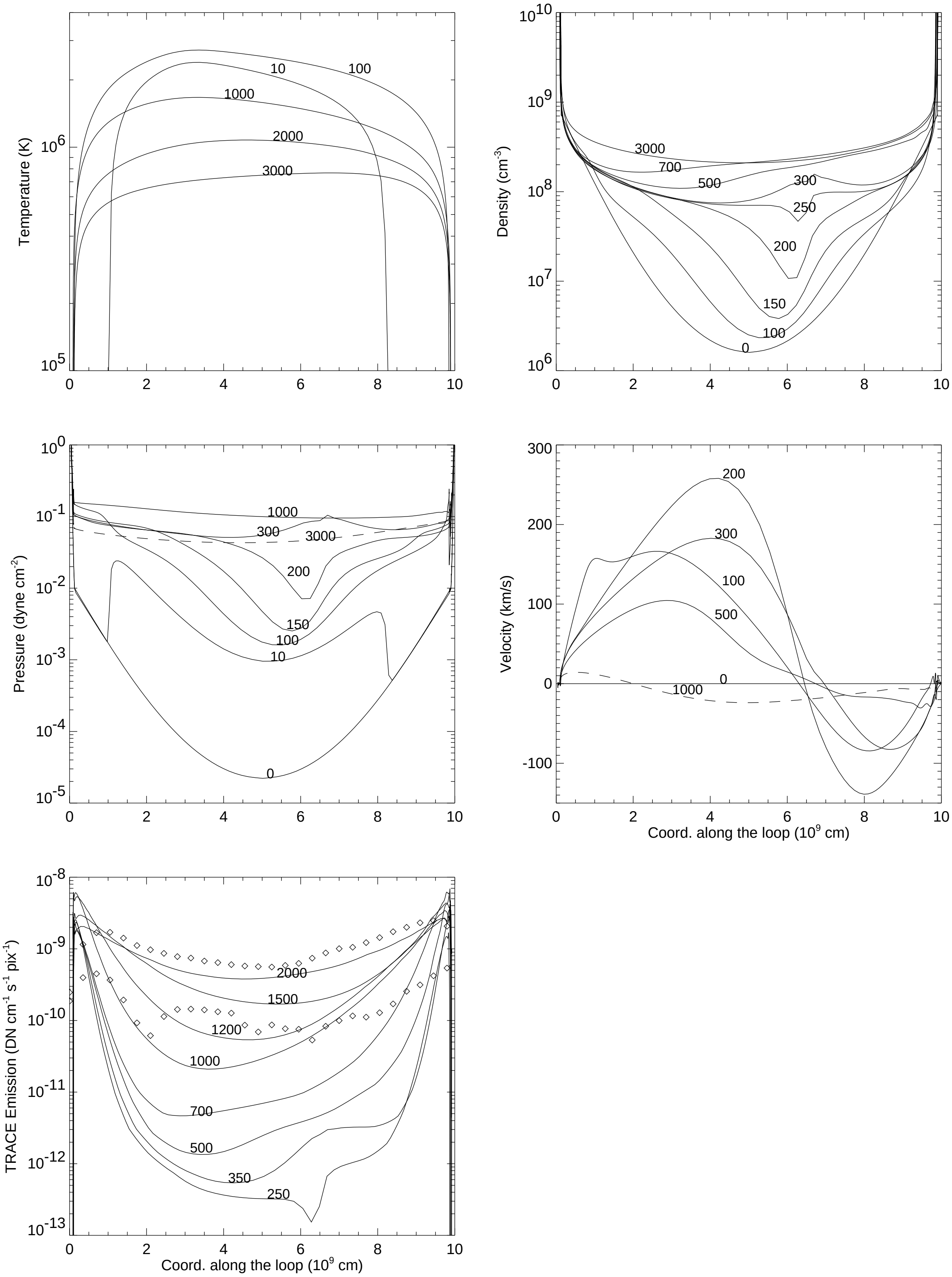

Figure 9. As Fig.7 for model loop C: the heating, on the right leg, is high and constant for 100 s and then exponentially decaying with an e-folding time 300 s. For a better readability the pressure at t = 3000 s is dashed (From Reale et al., 2000b).